Large-Scale *Ab Initio* Isobaric–Isothermal Simulations Using Self-Consistent van der Waals Inclusive Density Functionals

Hsin-Yu Ko[1] Biswajit Santra[1] Robert A. DiStasio Jr.[12] Roberto Car[1]

[1]Department of Chemistry, Princeton University, Princeton, NJ 08544, USA
[2]Department of Chemistry and Chemical Biology, Cornell University, Ithaca, NY 14853, USA

Introduction

- Common **Density Functional Theory** (DFT) functionals do not include the non-local correlation effects that underlie van der Waals (vdW) or dispersion interactions, leading to serious errors for weakly bound systems.
- For systems with hydrogen bonds, the self-interaction error (SIE) of DFT is sizeable and hybrid DFT functionals can be utilized to alleviate this error.
- Here, we report a general-purpose self-consistent (SC) implementation of vdW-inclusive DFT functionals and discuss their effects on the equilibrium properties of several systems.

Effects of SC vdW on electronic structure

- The long-range vdW energy (E_{vdW}) typically represents a tiny fraction ($\sim 0.001\%$) of the total energy; hence, its influence on electronic properties are typically ignored.
- Utilizing SC vdW, we have found large effects on the electron density $n(r)$ of molecular dimers, alkali-metal dimers, transition-metal surfaces, and organic-metal interfaces [1].
- Methodology: modified Kohn-Sham effective potential [2].

$$v[n(r)] = v_{GGA/hybrid}[n(r)] + \frac{\delta E_{vdW_{SC}^{TS}}[n(r)]}{\delta n(r)}$$

$$E_{vdW_{SC}^{TS}}[n(r)] = -\sum_{A<B} f_{damp}^{AB}[n(r)] \frac{C_{6AB}[n(r)]}{R_{AB}^6}$$

- vdW inclusive functionals are implemented in FHI-AIMS [3] and Quantum ESPRESSO (QE) [4].

Metal	PBE	PBE+vdW$_{SC}^{surf}$	Expt.
Cu	4.89	4.95	4.94
Rh	5.26	5.55	5.60
Ag	4.44	4.74	4.74

Table 1: Work functions (in eV) of various metal (111) surfaces obtained from experiment and theory.
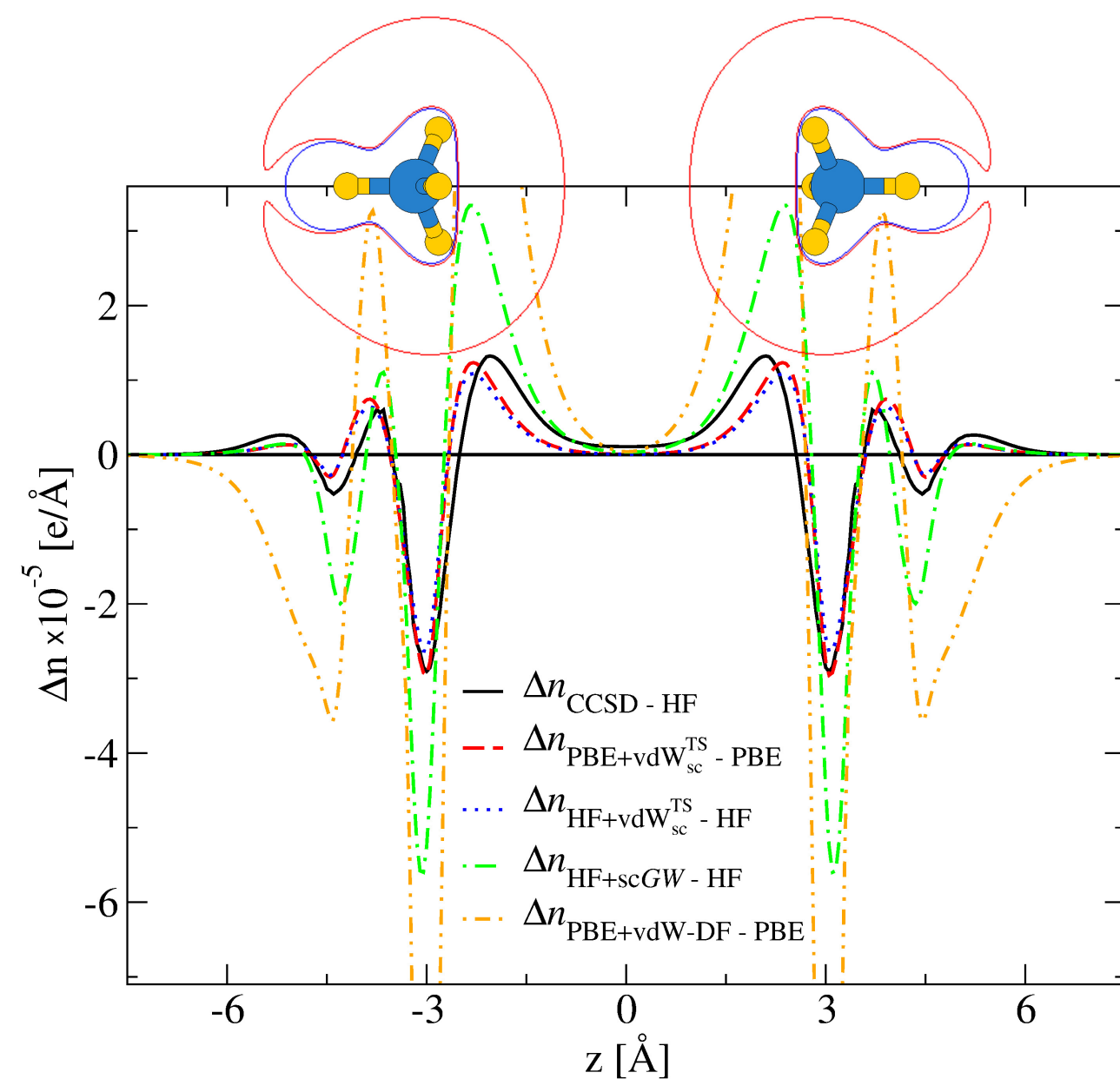

Figure 1: Integrated electron density differences [$\Delta n(r)$] for the methane (CH_4) dimer separated by a C-C distance of 6.72 Å along the z axis.

Role of vdW and anharmonicity on the equilibrium structures of molecular crystals
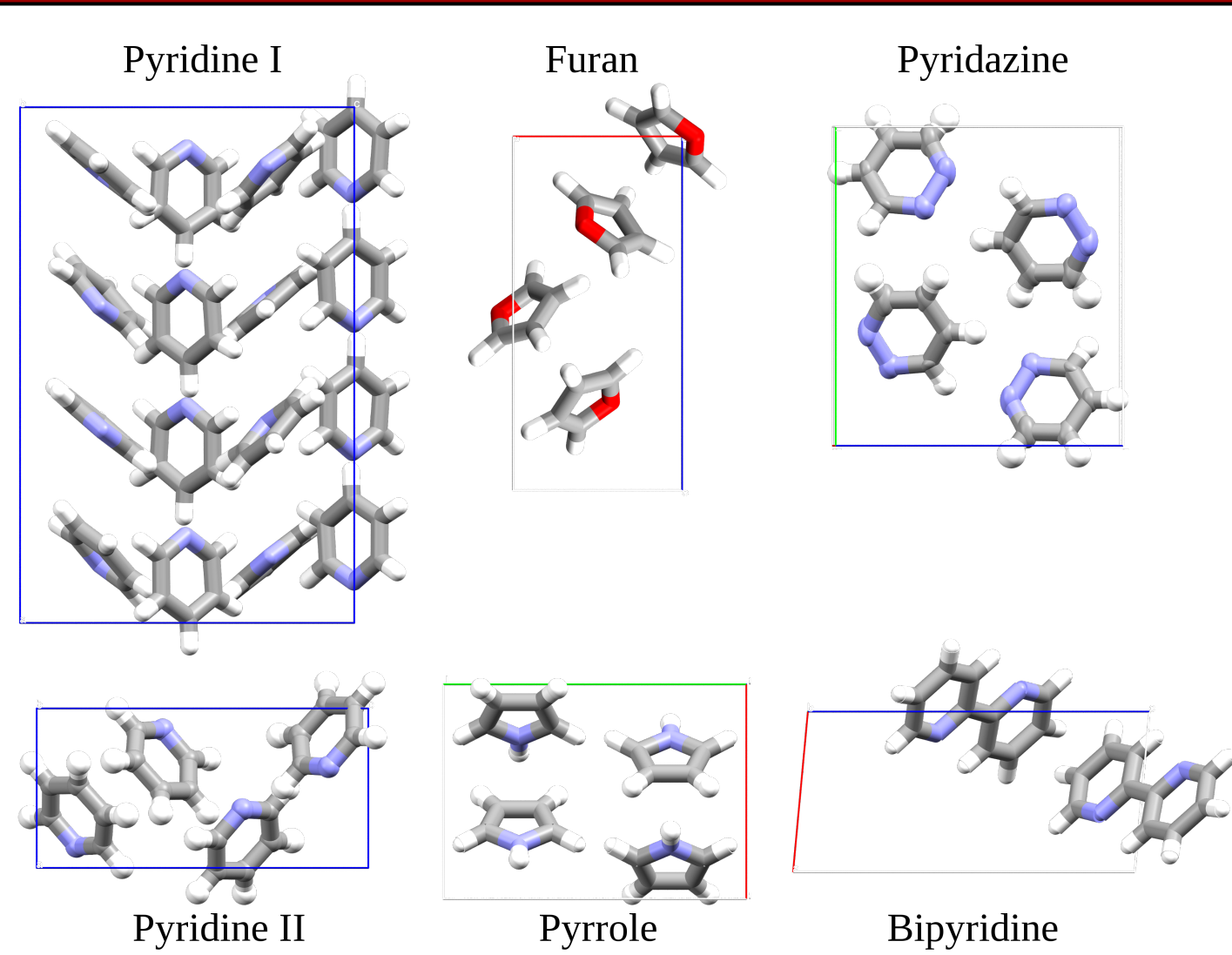

Figure 2: Pyridine polymorphs and **pyridine-like molecular crystals** (PLMCs)

- The pyridine molecule has a dipole of 2.3 D (theory) and 2.2 D (experiment) in the gas phase. We found that the molecular crystal arrangement minimizes the dipolar interaction energy.
- ***NpT*** dynamics captures anharmonicity and the SC vdW contribution to the stress tensor has been implemented in QE.
- The anharmonicity is large (with the PBE+vdW$_{SC}^{TS}$ pyridine volume at $T = 153$ K $\sim 4\%$ larger than at $T = 0$ K). Classical simulations seem to be sufficient to capture the anharmonicity in this system.
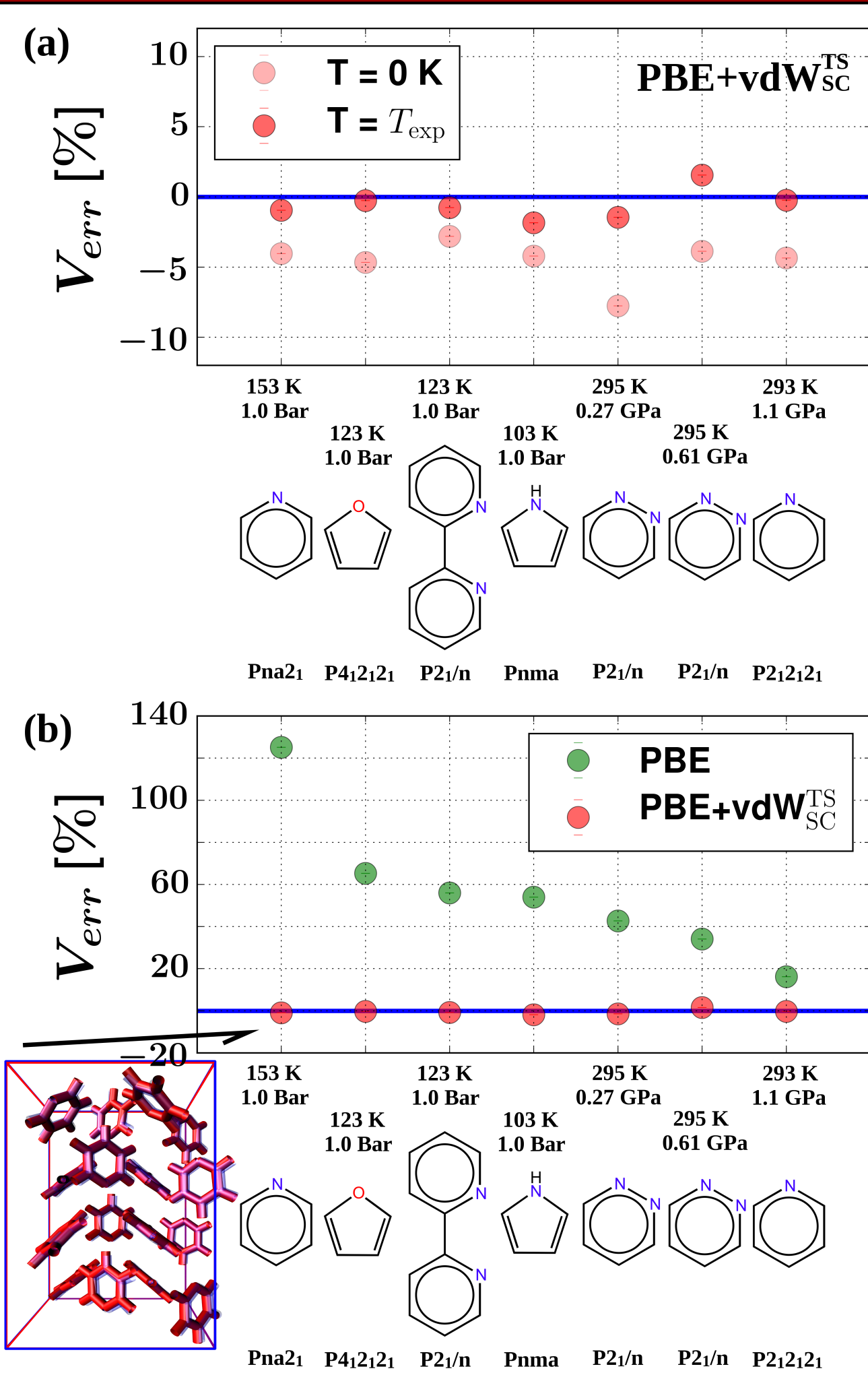

Figure 3: (a) PLMC structures from AIMD at p_{exp} and both $T = 0$ K and $T = T_{exp}$. (b) PLMC structures from AIMD at p_{exp} and T_{exp} with and without vdW. The inset shows an overlay of the calculated equilibrium structure with the experimental X-ray structure.

Nuclear quantum effects in pyridine I

- **Nuclear quantum effects** (NQE) in pyridine I were investigated with **Path-Integral** (PI-AIMD) using the QE + i-PI implementation [6].

Nuclei	Volume [Å³/molec]	Volume Error	KE [eV/molec]	EKE [eV/molec]
Classical	110.4	-0.99%	0.22	–
Quantum	111.6	0.11%	1.19	0.97

Table 2: Equilibrium volumes and ionic kinetic energies (KE) from AIMD and PI-AIMD at the experimental thermodynamic conditions. Colored-noise generalized Langevin thermostats (with a Trotter dimension of 8) were used in all PI-AIMD simulations.

- The calculated equilibrium volume including NQE is very close to the AIMD volume at p_{exp} and T_{exp}, in spite of the large excess ionic kinetic energy (EKE).
- NQE are sizeable in the intramolecular motions but small in the intermolecular motions; **equilibrium volumes** are primarily determined by **intermolecular motions**.
- To lowest-order in $\hbar$, NQE in the intermolecular motions are equivalent to the addition of a ΔT correction to the simulation temperature T,

$$\Delta T = \frac{\hbar^2}{36 M T^2} \left\langle \left| \vec{F} \right|^2 \right\rangle. \quad (1)$$

Here, M is the mass of one pyridine molecule and $\vec{F}$ is the force on its **center of mass**.

	T	ΔT
Pyridine I	153	6.8
Pyridine II	293	5.5

Table 3: Quantum temperature corrections (ΔT in Kelvin) using (1).

- The small magnitudes of ΔT reveal the **quasi-classical** character of the intermolecular motions at T_{exp}.

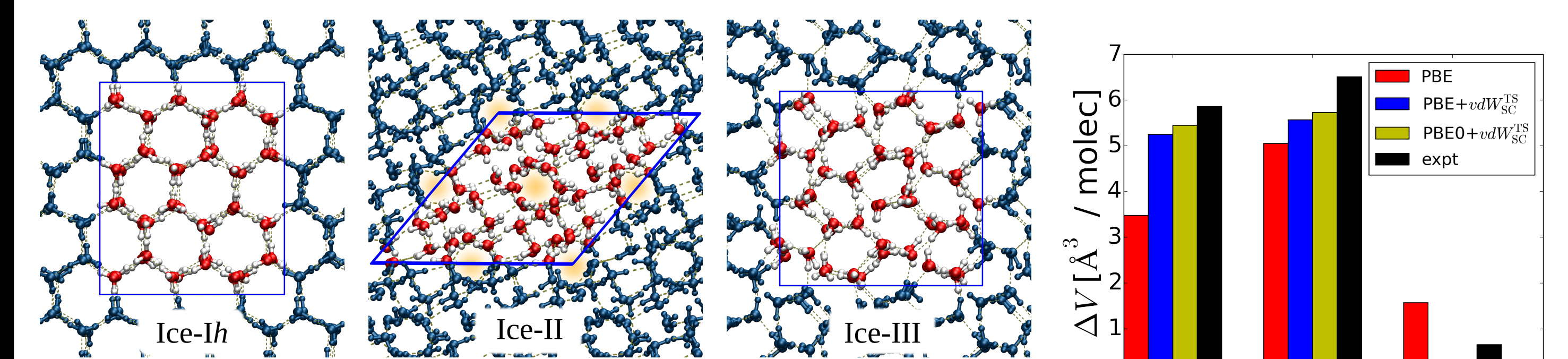## Ice triple point with PBE0+vdW$_{SC}^{TS}$

Figure 4: Snapshots of ice Ih, II, and III at the experimental triple point (0.21 GPa and 238 K).

- These large-scale ***NpT*** simulations were made possible by the linear-scaling exact exchange (EXX) and vdW algorithms implemented in QE [7]. The implementation uses analytical EXX stress tensors.
- Triple point properties calculated improved systematically from PBE to PBE+vdW$_{SC}^{TS}$ and to PBE0+vdW$_{SC}^{TS}$.
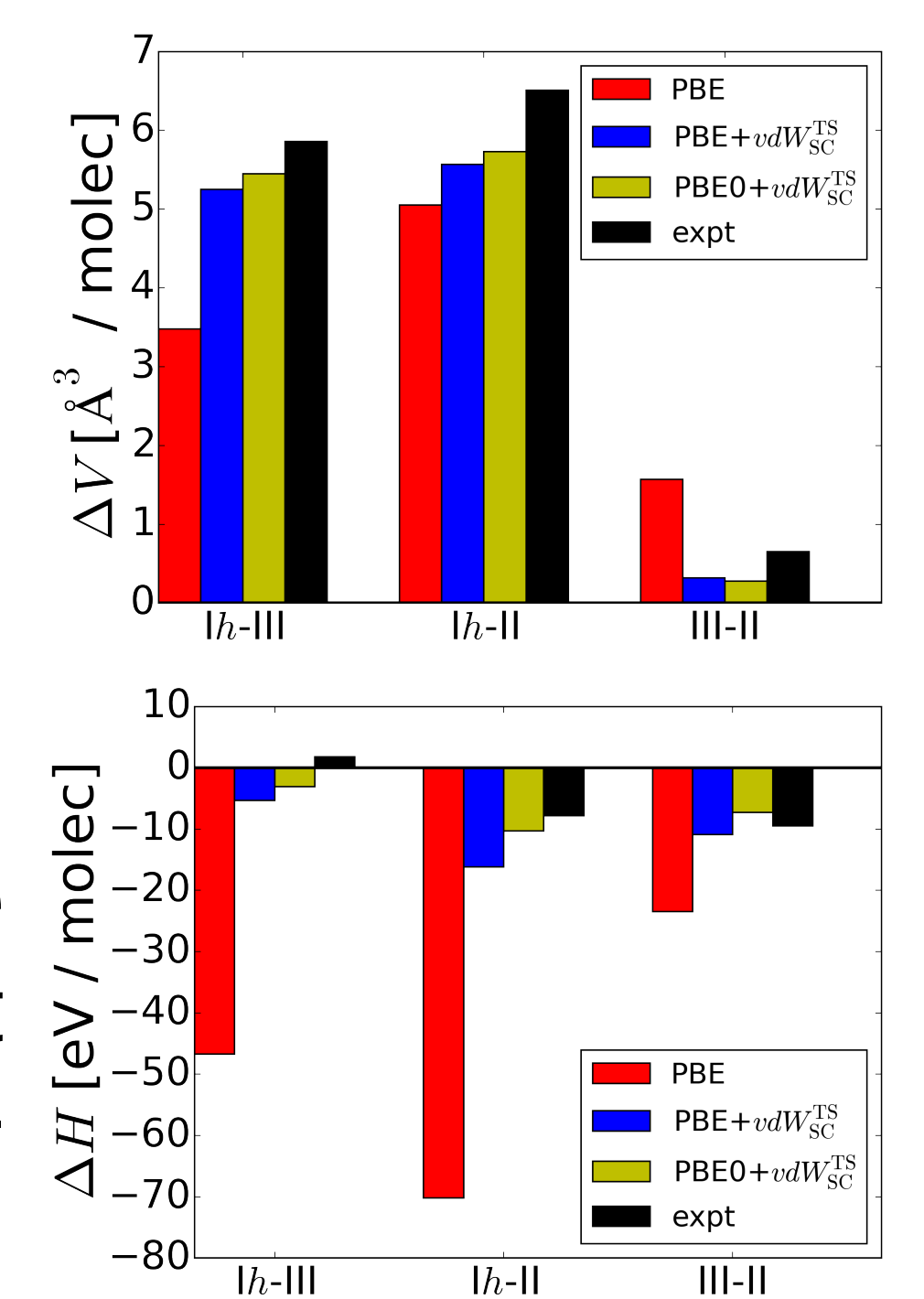

Figure 5: Volume (ΔV) and enthalpy (ΔH) differences between the ice phases at the triple point.

Conclusions

- In this work, we have provided a general-purpose implementation of vdW-inclusive DFT functionals for variable-cell ***NpT*** AIMD simulations and report their successful application to a wide variety of systems of interest in biology, chemistry, and physics.

References and acknowledgements

[1] N Ferri, R A DiStasio Jr, A Ambrosetti, R Car, A Tkatchenko, Phys. Rev. Lett. **114**, 176802 (2015). [2] A Tkatchenko, M Scheffler, Phys. Rev. Lett. **102**, 073005 (2009). [3] V Blum, *et al.*, Comput. Phys. Commun. **180**, 2175 (2009). [4] P Giannozzi, *et al.*, J. Phys.: Condens. Matter **21**, 395502 (2009). [5] R A DiStasio Jr, B Santra, Z Li, X Wu, R Car, J. Chem. Phys. **141**, 084502 (2014). [6] M Ceriotti, J More, D E Manolopoulos, Comput. Phys. Commun. **185**, 1019 (2014). [7] H-Y Ko, B Santra, R A DiStasio Jr, L Kong, Z Li, X Wu, R Car, (in preparation).